Supplement of Geosci. Model Dev., 7, 2503–2516, 2014
http://www.geosci-model-dev.net/7/2503/2014/
doi:10.5194/gmd-7-2503-2014-supplement

Geoscientific Model Development
Open Access

Supplement of

Sensitivity of aerosol radiative effects to different mixing assumptions in the AEROPT 1.0 submodel of the EMAC atmospheric-chemistry–climate model

K. Klingmüller et al.

Correspondence to: K. Klingmüller (klingmueller@cyi.ac.cy)

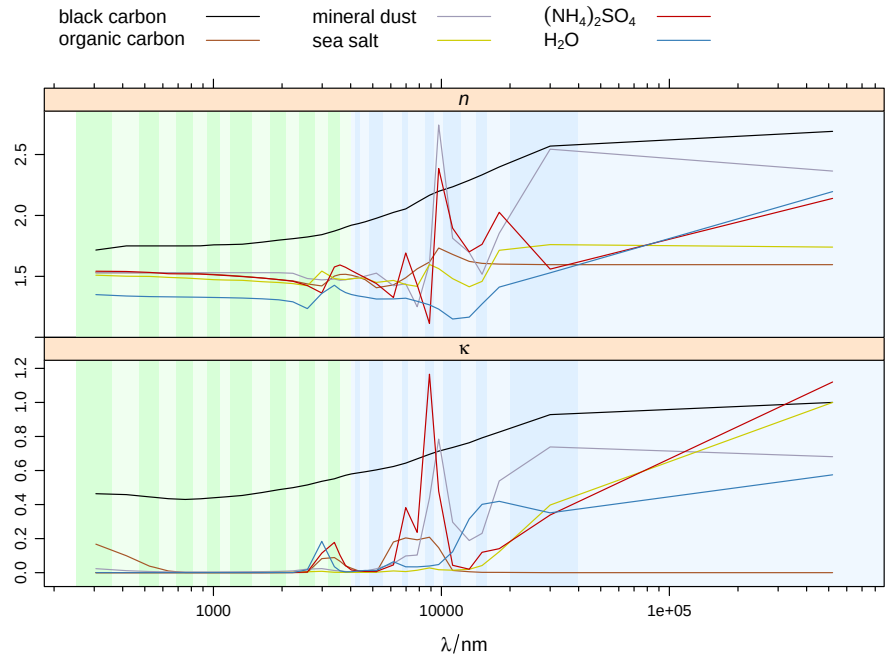

Figure S1: Real part n and imaginary part κ of refractive indices of various components used by the column model in section 4.1. The data for ammonium sulphate ($(NH_4)_2SO_4$) also serves as default for other components. The background shading represents the shortwave (green, including the AEROPT sub-bands) and longwave (blue) bands used in EMAC.

Refractive indices

Figure S1 shows refractive indices collected from the OPAC 3.1 database (Hess et al., 1998) (black carbon, mineral dust) and the HITRAN 2004 database (Rothman et al., 2005) (organic carbon, sea salt, ammonium sulphate, water). The mineral dust values have been complemented by data for $\lambda > 2.5$ μm from I. N. Sokolik (unpublished data, 2005), the organic carbon values by data for $\lambda < 0.7$ μm from Kirchstetter et al. (2004). The numerical values of the refractive indices can be found in Tab. S1 (real part n) and Tab. S2 (imaginary part κ).

References

Hess, M., Koepke, P., and Schult, I.: Optical Properties of Aerosols and Clouds: The Software Package OPAC., Bulletin of the American Meteorological Soci-

Table S1: Real part n of the refractive indices displayed in Fig. S1 for the shortwave (top) and longwave (bottom) bands.

λ/μm	n					
	BC	OC	Dust	SS	$(NH_4)_2SO_4$	H_2O
0.25 – 0.36	1.72	1.53	1.53	1.51	1.54	1.35
0.36 – 0.47	1.75	1.53	1.53	1.50	1.54	1.34
0.47 – 0.58	1.75	1.53	1.53	1.50	1.53	1.33
0.58 – 0.69	1.75	1.53	1.53	1.49	1.52	1.33
0.69 – 0.81	1.75	1.53	1.53	1.49	1.52	1.33
0.81 – 0.94	1.75	1.52	1.53	1.48	1.52	1.33
0.94 – 1.06	1.76	1.52	1.53	1.47	1.51	1.33
1.06 – 1.19	1.76	1.51	1.53	1.47	1.51	1.33
1.19 – 1.49	1.76	1.50	1.53	1.47	1.50	1.32
1.49 – 1.78	1.78	1.49	1.53	1.46	1.49	1.32
1.78 – 2.08	1.80	1.47	1.53	1.45	1.47	1.31
2.08 – 2.38	1.81	1.46	1.53	1.44	1.46	1.29
2.38 – 2.78	1.82	1.44	1.48	1.42	1.42	1.24
2.78 – 3.19	1.84	1.42	1.47	1.54	1.36	1.36
3.19 – 3.59	1.87	1.50	1.48	1.48	1.58	1.43
3.59 – 4.00	1.90	1.52	1.47	1.47	1.57	1.37
3.3 – 3.8	1.89	1.52	1.47	1.48	1.59	1.39
3.8 – 4.2	1.92	1.51	1.48	1.48	1.55	1.35
4.2 – 4.4	1.93	1.49	1.49	1.49	1.52	1.34
4.4 – 4.8	1.95	1.47	1.50	1.48	1.49	1.33
4.8 – 5.6	1.98	1.41	1.53	1.45	1.44	1.31
5.6 – 6.8	2.02	1.43	1.42	1.47	1.33	1.31
6.8 – 7.2	2.05	1.49	1.44	1.43	1.69	1.32
7.2 – 8.5	2.11	1.56	1.25	1.42	1.43	1.30
8.5 – 9.3	2.17	1.62	1.60	1.60	1.11	1.27
9.3 – 10.2	2.20	1.73	2.74	1.56	2.39	1.23
10.2 – 12.2	2.23	1.68	1.81	1.48	1.90	1.15
12.2 – 14.3	2.29	1.62	1.70	1.41	1.70	1.17
14.3 – 15.9	2.33	1.61	1.52	1.46	1.76	1.27
15.9 – 20.0	2.40	1.60	1.85	1.71	2.03	1.41
20.0 – 40.0	2.57	1.60	2.54	1.76	1.56	1.53
40.0 – 1000.0	2.69	1.60	2.36	1.74	2.14	2.20

Table S2: Imaginary part κ of the refractive indices displayed in Fig. S1 for the shortwave (top) and longwave (bottom) bands.

λ/μm	κ					
	BC	OC	Dust	SS	$(NH_4)_2SO_4$	H_2O
0.25 – 0.36	0.46	0.17	0.024	2.1e-06	1.0e-07	1.7e-08
0.36 – 0.47	0.46	0.099	0.012	7.0e-08	1.0e-07	2.4e-09
0.47 – 0.58	0.44	0.038	0.0066	1.4e-08	1.0e-07	2.1e-09
0.58 – 0.69	0.43	0.0098	0.0045	3.8e-08	1.0e-07	1.7e-08
0.69 – 0.81	0.43	0.00099	0.0040	1.1e-06	1.2e-07	1.4e-07
0.81 – 0.94	0.43	0.00086	0.0040	2.8e-05	3.6e-07	8.1e-07
0.94 – 1.06	0.44	0.00077	0.0041	0.00014	1.3e-06	3.1e-06
1.06 – 1.19	0.45	0.00067	0.0045	0.00026	6.1e-06	1.3e-05
1.19 – 1.49	0.45	0.00051	0.0052	0.00043	3.1e-05	5.0e-05
1.49 – 1.78	0.47	0.00028	0.0061	0.00068	7.6e-05	1.0e-04
1.78 – 2.08	0.49	6.3e-05	0.0074	0.00097	0.00065	0.00069
2.08 – 2.38	0.50	8.2e-05	0.011	0.0020	0.0010	0.00068
2.38 – 2.78	0.52	0.0014	0.021	0.0053	0.0040	0.017
2.78 – 3.19	0.54	0.082	0.024	0.0079	0.11	0.18
3.19 – 3.59	0.55	0.089	0.013	0.0021	0.18	0.035
3.59 – 4.00	0.57	0.040	0.0067	0.0014	0.042	0.0045
3.3 – 3.8	0.56	0.067	0.010	0.0016	0.10	0.011
3.8 – 4.2	0.58	0.026	0.0044	0.0014	0.016	0.0055
4.2 – 4.4	0.59	0.011	0.0054	0.0014	0.0097	0.010
4.4 – 4.8	0.59	0.0050	0.0092	0.0017	0.0072	0.013
4.8 – 5.6	0.60	0.0022	0.023	0.0029	0.0072	0.013
5.6 – 6.8	0.62	0.18	0.054	0.010	0.045	0.064
6.8 – 7.2	0.64	0.20	0.098	0.0064	0.38	0.034
7.2 – 8.5	0.67	0.19	0.10	0.014	0.24	0.034
8.5 – 9.3	0.70	0.21	0.44	0.028	1.2	0.039
9.3 – 10.2	0.71	0.15	0.78	0.017	0.48	0.048
10.2 – 12.2	0.74	0.013	0.30	0.014	0.043	0.12
12.2 – 14.3	0.76	0.0054	0.19	0.019	0.020	0.32
14.3 – 15.9	0.79	0.0018	0.23	0.042	0.12	0.40
15.9 – 20.0	0.83	0.0016	0.54	0.12	0.14	0.42
20.0 – 40.0	0.93	0	0.74	0.40	0.34	0.35
40.0 – 1000.0	1.0	0	0.68	1.0	1.1	0.57

ety, 79, 831–844, doi:10.1175/1520-0477(1998)079<0831:OPOAAC>2.0.CO;2, URL http://adsabs.harvard.edu/abs/1998BAMS...79..831H, 1998.

Kirchstetter, T. W., Novakov, T., and Hobbs, P. V.: Evidence that the spectral dependence of light absorption by aerosols is affected by organic carbon, Journal of Geophysical Research: Atmospheres, 109, doi:10.1029/2004JD004999, URL http://adsabs.harvard.edu/abs/2004JGRD..10921208K, 2004.

Rothman, L. S., Jacquemart, D., Barbe, A., Chris Benner, D., Birk, M., Brown, L. R., Carleer, M. R., Chackerian, C., Chance, K., Coudert, L. H., Dana, V., Devi, V. M., Flaud, J.-M., Gamache, R. R., Goldman, A., Hartmann, J.-M., Jucks, K. W., Maki, A. G., Mandin, J.-Y., Massie, S. T., Orphal, J., Perrin, A., Rinsland, C. P., Smith, M. A. H., Tennyson, J., Tolchenov, R. N., Toth, R. A., Vander Auwera, J., Varanasi, P., and Wagner, G.: The HITRAN 2004 molecular spectroscopic database, Journal of Quantitative Spectroscopy and Radiative Transfer, 96, 139, doi:10.1016/j.jqsrt.2004.10.008, URL http://adsabs.harvard.edu/abs/2005JQSRT..96..139R, 2005.